IEEE Access
Multidisciplinary | Rapid Review | Open Access Journal

Received June 4, 2019, accepted June 20, 2019, date of publication June 27, 2019, date of current version July 11, 2019.

Digital Object Identifier 10.1109/ACCESS.2019.2924696

Dynamic Adaptive Hybrid Impedance Control for Dynamic Contact Force Tracking in Uncertain Environments

HONGLI CAO[1], XIAOAN CHEN[2], YE HE[2], AND XUE ZHAO[1]
[1]College of Mechanical Engineering, Chongqing University, Chongqing 400044, China
[2]State Key Laboratory of Mechanical Transmission, Chongqing University, Chongqing 400044, China

Corresponding author: Xiaoan Chen (xachen@cqu.edu.cn)

This work was supported in part by the National NSF of China under 51475054 and Grant 51005259, and in part by the National Key R&D Program of China under Grant 2017YFB1301400.

ABSTRACT The importance of robot contact operation control has been increasing recently due to a need for robots to interact more with the outside world. However, traditional robot compliance control cannot take both transient contact force overshoots and steady-state force tracking error problems into account. To address this problem, this paper aims to design a dynamic adaptive hybrid impedance (DAHI) controller to deal with dynamic contact force tracking in uncertain environments (e.g., polishing scenarios). Under the premise of analyzing the transient response and steady-state error in the hybrid impedance control (HI) and adaptive hybrid impedance (AHI) control, the DAHI control, which combines the advantages from HI and AHI control, is applied to improve the performance of AHI controller. The main goal of such a controller is to avoid force overshoots in the contact stage while maintaining force tracking error in the dynamic tracking stage. The proposed controller is capable of adapting its update rate parameter online in order to track a reference force in uncertain environments. Besides, it does not require any modeling or estimation of an environment's dynamics or the robot's dynamics. The simulation and experimental results both show the achieved control performance. The results have also been compared with the previous control methods.

INDEX TERMS Contact operation control, dynamic adaptive hybrid impedance control, force tracking, force overshoots avoidance, industrial application.

I. INTRODUCTION

With the development of robot technology, contact operation is becoming an important area of robot application. When the end effector of a robot manipulator is in contact with an environment, the dynamic coupling between a manipulator and the environment generates reaction forces that must be handled properly to avoid the undesired effects that may directly lead to a task failing, even more serious consequences (manipulated object or manipulator itself damaged). Typical application scenarios include assembly [1]–[3], precise surface handling or processing (e.g., polishing) [4]–[6], surgical robot [7] and human-robot interaction [8], [9], among others.

Robot compliant control is proposed to resolve both position control and force control in order to solve the contact problem. The fundamental robot compliant control, which relies on the relationship between position and force, can be further classified as impedance control and hybrid position/force control. Hybrid position/force control was proposed by Raibert and Craig [10] and then developed by Mason [11]. It is based on formal models of the manipulator and task geometry which divides the task space into two domains: the position and force subspaces. Since it is not possible to control both position and force along the same degree of freedom, it tracks force and position in different directions, and this is considered to be the main drawback to this strategy. Specifically, Hogan [12]–[14] suggested a method to face this dynamic issue based on controlling the relationship between position and force: classical impedance control. The idea behind impedance control is the regulation of the mechanical impedance of the manipulator. Classical impedance control deals with the dynamic relationship between force and motion, hence it can control both motion and force simultaneously in one direction. In many cases, impedance control

The associate editor coordinating the review of this manuscript and approving it for publication was Yongping Pan.

outperformed the hybrid position/force control in terms of controlling the dynamic contact between manipulators and the environment, as well as showing more robustness in an unknown stiffness environment [15]. However, due to the easy implementation of the hybrid force/position control and superior dynamic force tracking performances, a variety studies have combined the concept of a hybrid force/position control and the impedance force scheme, i.e. a hybrid impedance (HI) control scheme [16], [17]. Hybrid impedance control is a combine of position control and impedance control. Impedance control itself can also achieve accurate ground force control and position control, but the need to adjust the impedance parameters, very troublesome and not intuitive. Therefore, better performance can be obtained by using hybrid impedance control. Nevertheless, due to the contact dynamic uncertainty of the environment, several research papers [18], [19] on the knowledge of contact dynamics were proposed to solve the major issue of the force tracking error.

It has been shown that the stability region of an impedance controller is enlarged through an adaptation law based on the real-time estimation of environmental parameters. Based on this work, the adaptive hybrid impedance (AHI) control was deemed to be a new stable force tracking impedance control scheme, capable of both tracking a desired force and of compensating for uncertainties in environment location and stiffness [20]–[24]. Moreover, due to most of the application robots being industrial robots that can only be controlled in position mode, several schemes were proposed to study the position-based impedance controller and to analyze performance and stability [25], [26]. Komati *et al.* [27] presented a new position-based impedance control scheme to estimate the environment, which was able to estimate the environment stiffness according to the past value of the position measurement.

Most previous research looking into non-deformed or slowly deformed environments focused more attention on theoretical analyses; however, it is difficult to realize this in practical industrial robots directly. Moreover, for a certain kind of processing, the parameters of the work piece (e.g., ultra-thin part, aircraft wings, patient's heart) are time-varying during operating process (e.g., polishing, cutting). Although, the AHI scheme has a superior performance in compensating force tracking error, force overshoot cannot be avoided. It is hard to maintain machining accuracy without damaging the parts. In order to identify an interaction controller analytically that avoids force overshoots, some researchers have taken the interaction control into account. Roveda *et al.* [28] proposed an analytical force overshoots free control architecture based on the estimation of the equivalent interacting elastic system stiffness for standard industrial manipulators. The method is then applied to the robot compliant base to avoid force overshoots [29]. Kanakis *et al.* [20] proposed a controller based on a priori bounded by user-defined bounds which is capable of establishing and maintaining the contact of the robot with a planar surface of an unknown stiffness and position. Sheng and Zhang [30] proposed a fuzzy adaptive hybrid impedance control scheme for the supporting side of a mirror milling system, which is capable of solving the force supporting problem with a time-varying environment stiffness. Despite of this, the issue of both maintaining the force tracking error and avoiding overshoots remains unresolved. Few researchers have considered both problems together, but only one aspect. Not only that, a simple and practical solution has not been presented to cope with industrial applications.

A. CONTRIBUTION

In view of this, the contribution of this paper validates the proposed dynamic adaptive hybrid impedance (DAHI) control for dynamic force tracking in uncertain environments. The main goal of such controller is to avoid the force overshoots in the contact stage while keeping force error in the dynamic tracking stage, where traditional control algorithms are not competent. Moreover, the DAHI is presented here mainly in order to cater to a time-varying environment, its adaptability to time-varying dynamic environments is far superior to traditional impedance control. The implementation of the proposed algorithm is easy and convenient in practical manufacture scenes where requiring force control based on industrial robots. It is expected that it would have a very significant impact on the film precision processing field for robot industrial applications.

B. OUTLINE

The paper is structured as follows. Section II reviews the classical compliance control algorithms, and the defects are exposed. The DAHI control scheme is proposed to solve the problem in Section III. Section IV presents the simulation results to verify the superiority of the proposed control algorithm. Experimental studies that verify the theoretical findings, are provided in Section V. Conclusions are presented in Section VI.

II. CONTACT MODEL AND COMPLIANT CONTROL

General Notation:

$M_d B_d K_d$:	the parameters are desired inertia, damping, and stiffness gains, respectively.
$P_e P_d P_c$:	the end-effector actual position, the desired position, the position command
$F_e F_d F$:	the contact force, the desired force, the control force
$z_e z_d z_c$:	the actual position, the desired position, the position command in z direction
$k\ (s)\ k_e k_d$:	second-order impedance model, environmental stiffness, desired stiffness
σ :	update rate
ρ :	compensation rate

In this section, the contact model between robot and environment is discussed. Then, the HI and AHI control with the force tracking strategy are presented. Finally, the comparison about transient and steady-state responses performance of the two controllers are analyzed.

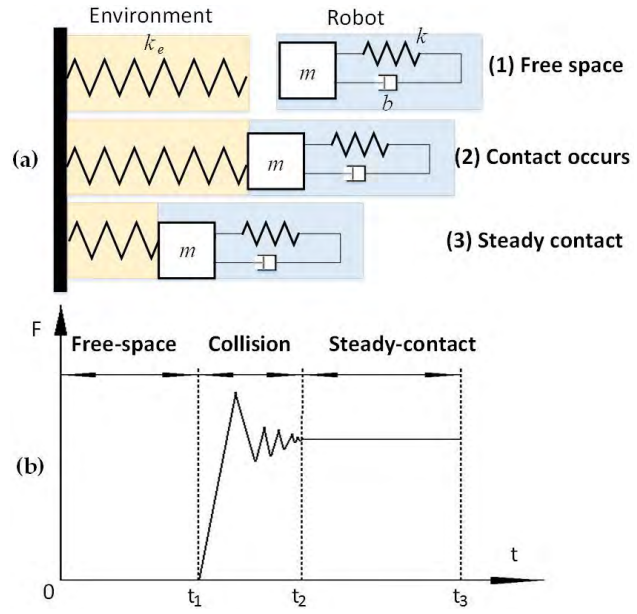

FIGURE 1. Contact model of robot and environment. (a) Description of the contact model, the environment and robot are a linear spring-mass-damping system. (b) Contact force varying of the robot from free space to steady contact space, which can be divided into three stage.

A. CONTACT MODEL

For modeling the contact force between robot and environment, the robot is represented by a second order mass–spring–damper system, and the environment is also represented by a spring system as in other literatures. Consider a single degree-of-freedom robot system in which a mass interacts with the environment (see Figure 1).

The contact model parameters are shown in Figure 1(a). Let m and x be the generalized inertia and displacement of the robot, respectively, and let F and F_{ext} be the control force and external force of the environment acting on the robot. Both F and F_{ext} are measured as positive in the direction of positive displacement. The equation of the motion of the robot can be written as follows:

$$m\ddot{x} = F - F_{ext} \tag{1}$$

As shown in Figure 1(b), from $0 - t_1$, there is no contact during the Free-space. From $t_2 - t_3$, the system will be stable after a process of collision which occurs in $t_1 - t_2$. Collision is inevitable and the collision time is transient, it will produce an extreme contact force during this period.

The force tracking for impendence control requires designing the driving force F that will establish the second-order relationship between force error and displacement error. In what follows, two commonly compliant control algorithms and the implementation will be introduced, namely the hybrid impedance control and the adaptive hybrid impedance control.

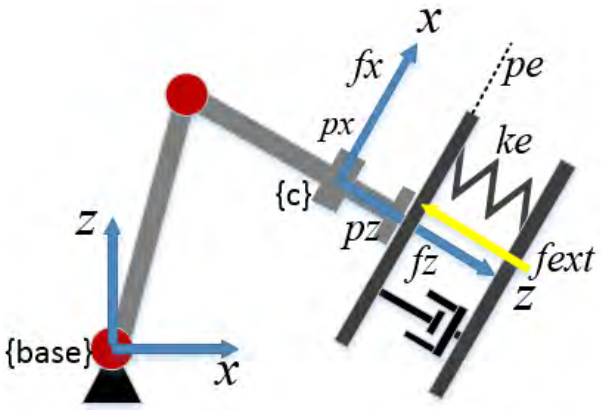

FIGURE 2. 2-Dof manipulator interacts with environment graphic representation. The force and position control directions are displayed in frame {c}.

B. HI CONTROL

In terms of the 2-dof manipulator, as shown in Figure 2, the coordinate system **{c}** is associated with the manipulator end-effector. Where f_x represents the force along the x axis, p_x is the position along x axis. The notification of the z axis is similar to the x axis. According to the analyses in the Figure 2, under the coordinate system **{c}**, the z axis is the direction of the force control, while position control is required along x axis. The position vector P and the force vector F can be denoted as:

$$P = [p_x \quad p_z] = [c_1 \quad 0] \tag{2}$$

$$F = [f_x \quad f_z] = [0 \quad c_2] \tag{3}$$

Therefore, put simply, the hybrid position/force and impedance controllers are combined to become a hybrid impedance (HI) control by a selection matrix S. By means of the compliance selection matrix, force control is only needed along the z axis. Therefore, the compliance selection matrix can be denoted as:

$$S = diag\,[1 \quad 0] \tag{4}$$

As shown in Figure 3, the hybrid impedance controller receives force error between the desired force and environment contact force in the z axis direction and then sends the displacement commands to a position-controlled robot to modify the position of end-effector in order to maintain a constant contact force.

Typically, the impedance model is chosen as a linear second-order system with such transfer-function $K(s) = 1/(Ms^2 + Bs + K)$, so the dynamic relationship between force tracking error ΔF and position perturbation E can be expressed as:

$$M_d \frac{d^2E(t)}{d^2t} + B_d \frac{dE(t)}{dt} + K_d E\,(t) = F_e - F_d = \Delta F \tag{5}$$

where $E\,(t) = P_d - P_e$, F_e denotes the actual force contact on the work piece, while F_d is the desired force. The perturbation

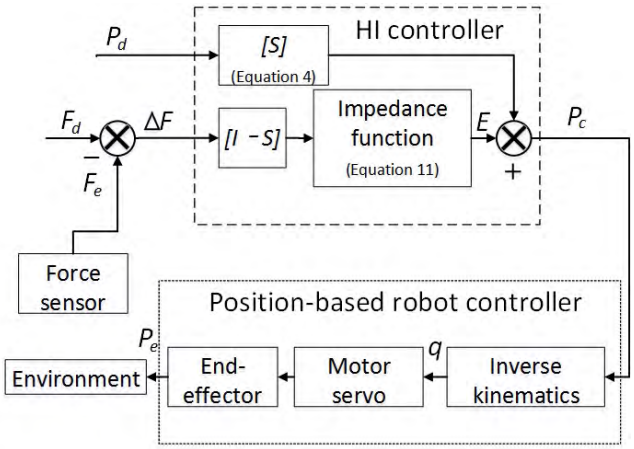

FIGURE 3. The implementation of the HI controller. Hybrid position and impedance control are combined to be hybrid impedance (HI) control by a selection matrix S.

E is used to modify the reference position trajectory P_d to produce the commanded trajectory $P_c = P_d + E = P_d + \Delta F \cdot K(s)$, which is then tracked by the position-based robot servo control system.

As we know, force control is only required along z axis. Taking just one dimension for analysis for the sake of simplify, the environment model is as following:

$$f_e = k_e (z_e - z_c) \tag{6}$$

where f_e is the force where the environmental deformation acted with the end-effector, k_e is the stiffness of the environment, z_e denotes the displacement of the environment. z_c is the commanded position which needs to be tracked in the z direction. To calculate the desired position trajectory z_d, the force tracking error can be obtained as:

$$\begin{aligned} \Delta f &= f_e - f_d = k_e (z_e - z_c) - f_d \\ &= k_e z_e - k_e (z_d + k(s) \Delta f) - f_d \end{aligned} \tag{7}$$

Substituting $k(s) = 1/(m_d s^2 + b_d s + k_d)$ into (7), yields:

$$\begin{aligned} &\Delta f (m_d s^2 + b_d s + k_d + k_e) \\ &\quad = (m_d s^2 + b_d s + k_d)[k_e(z_e - z_d) - f_d] \end{aligned} \tag{8}$$

At a steady state, (8) defines the steady state force tracking error. The steady-state force tracking error is obtained from (8) as:

$$\Delta f_{ss} = \lim_{s \to 0} s \Delta F(s) = \frac{k_d}{k_d + k_e} [k_e (z_e - z_d) - f_d] \tag{9}$$

This makes the steady state force tracking error asymptotically stable. From (9), the reference position or the desired stiffness must satisfy one of the following conditions:

$$\begin{cases} z_d = z_e - \dfrac{f_d}{k_e} \\ k_d = 0 \end{cases} \tag{10}$$

Equation (10) shows that if the precise location of the environment z_e and the exact value of the environment stiffness k_e are known, the desired position trajectory z_d can be computed according to (10) to exert the desired contact force f_d on the environment. However, in practice the values of z_e and k_e are not known in advance; it is difficult to directly compensate the environment location and stiffness because the environment parameters are time-varying. There will be an infinite steady-state force tracking error because the force error will always exist. Hoverer, (10) also suggests that setting the stiffness gain k_d to zero will satisfy the ideal steady state condition in any situation stiffness k_e. Therefore, relying on (10), the impendence function in (5) for the z axis can be rewritten as:

$$m_d \ddot{e} + b_d \dot{e} = \Delta f \tag{11}$$

C. AHI CONTROL

In the practical system, the stiffness of environment k_e is a continuous time-varying variable. A force tracking error cannot be avoided due to the changeable environment stiffness k_e gain. Even worse, the robot servo system or force sensor have transmission delays, measurement noises and model uncertainties. There will be an infinite steady-state force tracking error. Therefore, HI is not competent for accurate force tracking control. In order to reduce the force tracking error, an improved adaptive algorithm based on HI control is proposed to address this issue in [17]. The adaptive hybrid impedance (AHI) algorithm is given by:

$$\Delta f = m \ddot{\hat{e}}(t) + b \left(\dot{\hat{e}}(t) + \rho \right) \tag{12}$$

where ρ is adjusted according to the force error online. The estimation of the environment location is $\hat{x}_e = x_e - \delta x_e$.The position error is then expressed as $\hat{e} = e + \delta x_e$. The adaptive compensating law of the force tracking error, i.e., ρ can be denoted as:

$$\rho(t) = \rho(t - T) + \sigma \frac{(f_d(t - T) - f_e(t - T))}{b} \tag{13}$$

In its initial state $\rho(0) = 0$, T is the sampling period of the system, and σ is the update rate. The update rate is a time-varying parameter associated with system stability. According to the Laplace transform of the AHI control law in (12), the displacement along the z axis is given by:

$$\Delta z = \frac{\Delta f + b_d \rho}{m_d s^2 + b_d s} \tag{14}$$

Based on the error of desired force as well as the adaptive law, the adaptive hybrid impedance control can maintain the constant desired force.

From an intuitive point of view for analyzing the compensation law, it can be seen that when the value of the update rate σ is large, the compensated effect will be more obvious (better force tracking ability), but the contact force will jitter in a larger scope (large force overshoots). Instead, when the value of the update rate σ is small, the compensated effect will be not obvious (worse force tracking ability), and the contact

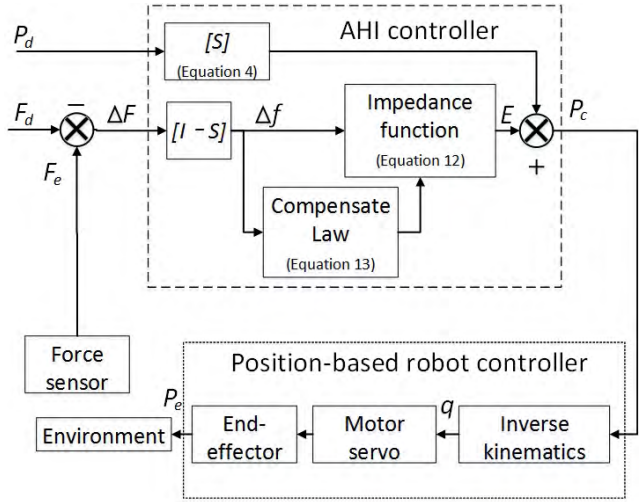

FIGURE 4. The implementation of AHI controller. Compared with HI, there is an adaptive compensation.

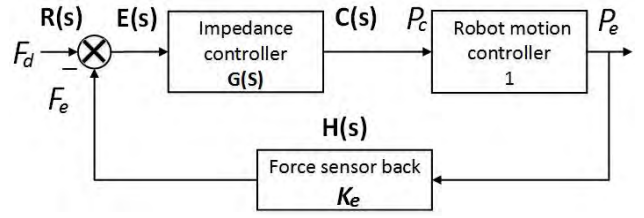

FIGURE 5. The transfer function of the interaction model. The robot motion controller has a superior position tracking ability, and is simplified as gain 1 here. The difference between the transient and steady-state transfer function of the impedance controller G(s) is that the compensation algorithm is a sum function of time for steady-state.

force will be a slower trend scope (small force overshoots). Besides, the HI is the special form of AHI if σ is equal to zero. In the following, the performance comparison about transient response and steady-state error of HI and AHI controllers are analyzed to explore the pros and cons.

D. PERFORMANCE COMPARISON

In general, industrial robots can achieve super position control ability, the model uncertainties (including inertia, friction and Coriolis, etc.) and some external disturbances can be suppressed by PID control or some compensation technologies, which means that $P_c = P_e$ (position tracking ability). The simple closed-loop control loop of the controller, robot and environment system is shown in Figure 5.

1) FORCE TRACKING COMPARISON

Rewriting (13) and marking $c(t) = f_d(t) - f_e(t)$. According to the principle of dispersion, n elements of the ρ series can be expanded as:

$$b\rho(t) = b\rho(t - nT) + \sigma c(t - nT) + \cdots + \sigma c(t - T) \tag{15}$$

When the initial state is zero. Combining (12) and (15) yields:

$$\begin{aligned}\Delta f &= m\ddot{\hat{e}}(t) + b\left(\dot{\hat{e}}(t) + \rho\right) \\ &= m\ddot{\hat{e}}(t) + b\dot{\hat{e}}(t) + \sigma\left(c(t - nT) + \cdots + c(t - T)\right)\end{aligned} \tag{16}$$

With the Laplace transform (16), the controller steady transfer function is:

$$\frac{\hat{e}(s)}{c(s)} = \frac{1 + \sigma(e^{-nTs} + \cdots + e^{-Ts})}{ms^2 + bs} \tag{17}$$

Under the assumption that n is a sufficiently large number, it can be expressed as:

$$\sum_{n=1}^{\infty} e^{-nTs} = \frac{e^{-Ts}}{1 - e^{-Ts}} \tag{18}$$

When the sampling rate T is sufficient, the delayed term can be approximated as $e^{-Ts} \cong 1 - Ts$ with the Taylor expansion. The controller steady transfer function (17) can be rewritten as:

$$G(s) = \frac{\hat{e}(s)}{c(s)} = \frac{1 + \sigma\frac{1-Ts}{Ts}}{ms^2 + bs} \tag{19}$$

The error transfer function $\Phi(s)$ for a closed-loop system is:

$$\Phi(s) = \frac{E(S)}{R(s)} = \frac{1}{1 + G(s)H(s)} \tag{20}$$

Because the environment has complex dynamic uncertainty, in order to analyze the steady-state error of the controller, suppose the input is a step $R(s) = 1/s$ and a slope signal $R(s) = 1/s^2$, the steady error of HI and the AHI controller are the following, respectively:

$$\begin{aligned}e_{ss} &= \lim_{s\to 0}\Phi(s)R(s) = \lim_{s\to 0}\Phi(s)(1/s) \\ &= \begin{cases}(HI) = \lim\limits_{s\to 0} s\dfrac{1}{1 + \frac{1}{ms^2+bs}k_e}\dfrac{1}{s} = 0 \\ (AHI) = \lim\limits_{s\to 0} s\dfrac{1}{1 + \frac{1+\sigma\frac{1-Ts}{Ts}}{ms^2+bs}k_e}\dfrac{1}{s} = 0\end{cases}\end{aligned} \tag{21}$$

$$\begin{aligned}e_{ss} &= \lim_{s\to 0}\Phi(s)R(s) = \lim_{s\to 0}\Phi(s)\left(1/s^2\right) \\ &= \begin{cases}(HI) = \lim\limits_{s\to 0} s\dfrac{1}{1 + \frac{1}{ms^2+bs}k_e}\dfrac{1}{s^2} = \dfrac{b}{k_e} \\ (AHI) = \lim\limits_{s\to 0} s\dfrac{1}{1 + \frac{1+\sigma\frac{1-Ts}{Ts}}{ms^2+bs}k_e}\dfrac{1}{s^2} = 0\end{cases}\end{aligned} \tag{22}$$

For more complex input, a sine signal $r(t) = sin\omega t$, long division method is used to compute dynamic error (take the first three terms):

$$\begin{aligned}e_{ss}(t) &= \Phi(0)r(t) + \dot{\Phi}(0)\dot{r}(t) + (1/2!)\ddot{\Phi}(0)\ddot{r}(t) + \cdots \\ &= \begin{cases}e_{ss}(HI) = \omega\dfrac{b}{k_e}cos\omega t - \omega^2\dfrac{mk - b^2}{2k_e^2}sin\omega t + \cdots \\ e_{ss}(AHI) = 0 - \omega^2\dfrac{bT}{k_e\sigma}sin\omega t + \cdots\end{cases}\end{aligned} \tag{23}$$

Through (21), (22) and (23), as the inputs are increasingly complex, AHI has been able to achieve small force tracking error, while HI has failed. Moreover, as σ increases, the dynamic error of AHI will decrease, which can be seen from (23). What's more, AHI has a certain inhibitory effect on the varying-stiffness dynamic environment, while HI cannot adapt.

2) FORCE OVERSHOOTS COMPARISON

For transient response analysis, the controller transfer function needs to be rewritten due to n no longer being an infinite number. Hence, the compensation of (13) is rewritten and both sides are divided by the sampling time:

$$\frac{\rho(t)-\rho(t-T)}{T}=\frac{\sigma}{b}\frac{f_d(t-T)-f_e(t-T)}{T} \tag{24}$$

Due to the initial state $\rho(0)=0$. When the sampling rate T is sufficient, it can be approximated that $c(t-T)\cong c(t)$. Therefore, a proportional relationship between ρ and c is:

$$\rho(t)=-\frac{\sigma}{b}c(t) \tag{25}$$

Substituting (25) into (12) then do Laplace transformation, the transient transfer function of the controller is:

$$G(s)=\frac{\hat{e}(s)}{c(s)}=\frac{1+\sigma}{ms^2+bs} \tag{26}$$

The transient transfer function $\Psi(s)$ for a closed-loop system is:

$$\Psi(s)=\frac{G(s)H(s)}{1+G(s)H(s)}=\frac{(1+\sigma)k_e}{ms^2+bs+(1+\sigma)k_e} \tag{27}$$

The damping coefficient ζ about the oscillation form of the controller can be calculated form (27) as:

$$\zeta=\frac{b}{2\sqrt{m(1+\sigma)k_e}} \tag{28}$$

In form (28), it can be clearly seen that as σ increases, the damping coefficient decreases, the system will present oscillating in contact stage. This indicates that HI has better vibration suppression than AHI.

Through the above transient and steady state analysis, it is not appropriate to keep the update rate unchanged. Therefore, in order to maintain a stable desired contact force (keeping force tracking error and avoiding force overshoots), the update rate σ needs to be adjusted online, so a dynamic controller is added. Then, a dynamic adaptive hybrid impedance (DAHI) control scheme is introduced in the following section.

III. DAHI CONTROL

The proposed controller contains an algorithm for calculating the update rate dynamically. In the following, two ways calculating the update rate are described.

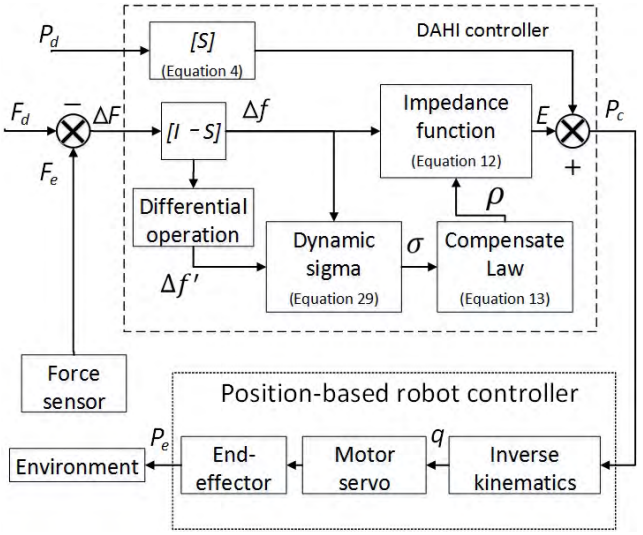

FIGURE 6. The implementation of the DAHI controller. Compared with AHI, there is a dynamic calculating σ.

A. DAHI ALGORITHM

According to the representation of AHI algorithm, this simple robust adaptive control scheme for a robot manipulator is used to compensate for uncertainties in an environment.

However, if σ is oversized, oscillation occurs. If σ is small, the force error grows larger. To improve the performance of AHI controller, in the DAHI controller, a dynamic calculating the update rate is introduced:

$$\begin{cases}\sigma=\dfrac{1}{\alpha|\Delta f|+\beta|\Delta f'|+U_{limt}}, & Recip\ mode\\ \sigma=\dfrac{1}{e^{\alpha|\Delta f|}+e^{\beta|\Delta f'|}+U_{limt}}, & Exp\ mode\end{cases} \tag{29}$$

The update rate σ is modified on-line using the feedback information: force error Δf and force error variation $\Delta f'$. Here, α, β are the gains which used to regulate the specific gravity of force error and force error variation. The selection needs further study. U_{limt} is the upper limit to guarantee the system in a stable state. To guarantee an asymptotically stable system, the update rate σ needs to be set in a small range.

Due to the ways in which the update rate are calculated, which are similar to the reciprocal ratio and exponent function, the names DAHI (Recip mode) and DAHI (Exp mode) are used for simple marking. The implementation of the whole controller is shown in Figure 6. The DAHI controller is proposed to compensate the force tracking error caused by changed environment stiffness, and to be certain that there is no force overshoots by adjusting σ. From an intuitive point of view, the DAHI combines the advantages of the HI and AHI controllers that are, small steps towards avoiding overshoot at a contact state and large steps towards achieving force tracking at a steady-state. In contrast, DAHI (Exp mode) has a wider update rate regulation range than DAHI (Recip mode).

B. STABILITY AND BOUNDARY ANALYSIS

In order to determine the value of the σ adjustable range, and at the same time its upper limit, a stability analysis is carried out.

Substituting (13) into (12), yields:

$$\begin{aligned} &f_e(t) - f_d(t) \\ &= m\overset{\approx}{e}(t) + b\hat{e}(t) + bp(t-T) + \sigma\left[f_d(t-T) - f_e(t-T)\right] \\ &= m\left[\ddot{e}(t) + \delta\ddot{x}_e(t)\right] + b\left[\dot{e}(t) + \delta\dot{x}_e(t)\right] \\ &\quad + bp(t-T) + \sigma\left[f_d(t-T) - f_e(t-T)\right] \end{aligned} \tag{30}$$

Reorganizing (30) yields:

$$\begin{aligned} &m\ddot{\hat{e}}(t) + b\ddot{\hat{e}}(t) + bp(t-T) + \sigma\left[f_d(t-T) - f_e(t-T)\right] \\ &\quad - \left[f_e(t) - f_d(t)\right] = -m\delta\ddot{x}_e(t) - b\delta\dot{x}_e(t) \end{aligned} \tag{31}$$

According to the stiffness model between the robot and the environment, which is $f_e = k_e(z_e - z_c) = -k_e e$, after the differential it becomes:

$$\dot{e} = -\dot{f}_e/k_e, \quad \ddot{e} = -\ddot{f}_e/k_e \tag{32}$$

Substituting (32) into (31), yields:

$$\begin{aligned} &-m\ddot{f}_e(t) - b\dot{f}_e(t) + bk_e p(t-T) - k_e\left[f_e(t) - f_d(t)\right] \\ &\quad \sigma k_e\left[f_d(t-T) - f_e(t-T)\right] = -m\delta\ddot{x}_e(t) - b\delta\dot{x}_e(t) \end{aligned} \tag{33}$$

Let $\hat{f}_e(t) = k_e\delta x_e(t)$, and then (33) could be represented as:

$$\begin{aligned} &m\left(\ddot{f}_d(t) - \ddot{f}_e(t)\right) + b\left(\dot{f}_d(t) - \dot{f}_e\right) + bk_e p(t-T) \\ &\quad + \sigma k_e\left[f_d(t-T) - f_e(t-T)\right] - k_e\left[f_e(t) - f_d(t)\right] \\ &\quad = m\left[\ddot{f}_d(t) - \hat{f}_e(t)\right] + b\left[\dot{f}_d(t) - \dot{\hat{f}}_e(t)\right] \end{aligned} \tag{34}$$

Marking $r(t) = f_d(t) - \hat{f}_e(t)$, (34) is rewritten as:

$$m\ddot{c} + b\dot{c} + bk_e p(t-T) + k_e c + \sigma k_e c(t-T) = m\ddot{r} + b\dot{r} \tag{35}$$

Combining (15) and (35) yields:

$$\begin{aligned} &m\ddot{c} + b\dot{c} + k_e c \\ &\quad + \sigma k_e(c(t-(n+1)T) + \cdots + c(t-T)) = m\ddot{r} + b\dot{r} \end{aligned} \tag{36}$$

Laplace transform of (36) is:

$$\frac{c(s)}{r(s)} = \frac{ms^2 + bs}{ms^2 + bs + k_e + \sigma k_e\left(e^{-(n+1)Ts} + \cdots + e^{-Ts}\right)} \tag{37}$$

The stability of (37) can be guaranteed by the characteristic as:

$$ms^2 + bs + k_e + \sigma k_e\left(e^{-(n+1)Ts} + \cdots + e^{-Ts}\right) = 0 \tag{38}$$

Under the assumption that n is a sufficiently large number, and that the sampling rate T is sufficient $e^{-Ts} \cong 1 - Ts$. Substituting (18) into (38):

$$mTs^3 + bTs^2 + k_e T(1-\sigma)s + \sigma k_e = 0 \tag{39}$$

According to the Routh criterion, the Routh array is presented as:

$$\begin{array}{lll} s^3 & mT & k_e T(1-\sigma) \\ s^2 & bT & \sigma k_e \\ s^1 & \dfrac{bk_e T^2(1-\sigma) - mk_e T\sigma}{bT} & 0 \\ s^0 & \sigma k_e & 0 \end{array} \tag{40}$$

To ensure the stability of the system, the coefficients of the first column and the coefficients of the characteristic equation must be positive, which is represented as:

$$\begin{cases} \dfrac{bk_e T^2(1-\sigma) - mk_e T\sigma}{bT} > 0 \\ k_e T(1-\sigma) > 0 \\ \sigma k_e > 0 \end{cases} \tag{41}$$

Simplifying (41), the boundary of σ is:

$$0 < \sigma < \frac{bT}{m + bT} \tag{42}$$

Substituting (42) into (29), yields:

$$\begin{cases} U_{limt} > \dfrac{m+bT}{bT} - (\alpha|\Delta f| + \beta|\Delta f'|), & Recip\ mode \\ U_{limt} > \dfrac{m+bT}{bT} - (e^{\alpha|\Delta f|} + e^{\beta|\Delta f'|}), & Exp\ mode \end{cases} \tag{43}$$

Thus, setting $U_{limit} = (m + bT)/bT$ for simple. For practice application, the upper value must be lager enough to ensure reliable stability (due to the model uncertainties and disturbances in practice), thus sacrificing some force tracking accuracy.

For a stable system, the steady-state error e_{ss} can be defined based on the Laplace transform. For convergence, the steady-state error can be calculated as:

$$\begin{aligned} e_{ss} &= \lim_{t\to\infty} e(t) = \lim_{s\to 0} sE(s) = \lim_{s\to 0} s(c(s) - r(s)) \\ &= \lim_{s\to 0} s\left[\frac{ms^2 + bs}{ms^2 + bs + k_e + \sigma k_e(e^{-(n+1)Ts} + \cdots + e^{-Ts})} r(s) - r(s)\right] \end{aligned} \tag{44}$$

When the input is a step function with the form as $r(s) = 1/s$. Equation (44) yields result:

$$e_{ss} = \lim_{s\to 0} s(c(s) - r(s)) = -1 \tag{45}$$

According to the (45), the following conclusion can be conclude:

$$\lim_{s\to 0} sc(s) = 0, \ \lim_{t\to\infty} c(t) = 0 \tag{46}$$

Therefore, when $t \to \infty, f_e \to f_d$. The contact force between robot and environment converges to the desired force. Actually, even if $r(s)$ is not a step function, like a slope or sine function as in simulation and experiment, the tracking error goes to zero is also can be proven.

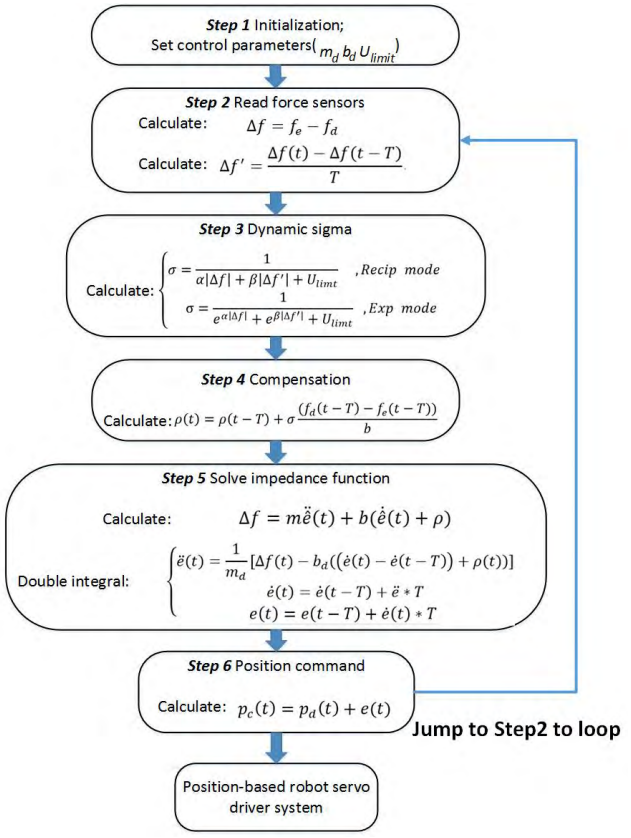

FIGURE 7. The algorithm for the DAHI controller. Step 2 to step 6 is a cycle loop (The cycle period is 4ms).

C. THE ALGORITHM IMPLEMENTATION OF DAHI

For convenient applying in industrial robots, the control algorithm should be discretized by sampling time. Figure 7 shows the implementation of the DAHI control algorithm.

The control algorithm begins by initializing and setting the constants, such as the impedance inertias, mass proprieties, upper limits, etc. The actual contact force is acquired from force sensor, then the force error Δf is calculated and the gradient of the force error $\Delta f'$ is obtained via difference calculation. Once the previous conditions are completed, the dynamic parameters update rate σ is calculated by (29). Then, the compensation force is calculated by (13). Double integrals are used to solve the second order differential equations (impedance transform), Figure 7 is the discretization form. Finally the position commands are calculated and then sent to the robot servo system. Now the whole cycle is complete, and repeats indefinitely. The whole control cycle period is 4ms.

IV. SIMULATION

To verify the proposed force tracking strategy and the theoretical analysis results, a series of simulation studies are conducted and presented in this section. The simulations include a variety of force tracking scenarios which basically cover most of the actual situations. The simulation platform is based on Matlab/Simulink which mainly consists of the following parts: the hybrid controllers (HI, AHI, and DAHI), dynamic environments, the force sensor noises, and the model uncurtains.

A. SIMULATION SETUP

To compare force overshoots and tracking error performance of the HI, AHI and DAHI controls in different environments. The basic impedance controller parameters $m_d = 1\ \mathrm{Ns^2/m}$ and $b_d = 200\ \mathrm{Ns/m}$ are selected based on experiences (Here refers to the benchmark). The calculation in simulation is using fixed step solver, the sample time $T = 4$ ms, and the force is step signal, the desired tracking force is $F_{desired} = 30$ N at steady state. Modeling uncertainty is introduced in both implementations by considering the estimated mass m'' instead of the mass $m = 1$ kg. The (PD) position controller is designed with high gains, which is common practice. To test the force tracking performance in a time–varying continuous stiffness environment, the environment stiffness is presented as:

$$k_e = 4000 + 200\sin\left(\frac{\pi}{2}t\right) \tag{47}$$

The unmolded friction F_f which is assumed to have a form with $c_v = 1\mathrm{Ns/m}$ and $F_c = 3$ N as the coefficients of viscous and coulomb friction:

$$F_f = -\,\mathrm{sign}(\dot{x})\,(c_v|\dot{x}| + F_c) \tag{48}$$

To study the impact of the AHI controller in the situation, the value of the update rate σ can be changed manually at two values for comparison, $\sigma = 0.01$ and $\sigma = 0.05$, which all in the stable range. Moreover, we can found that HI is a special form of AHI when $\sigma = 0$. To ensure stability and contrast, the dynamic σ of the DAHI controller is set a range of 0 to 0.05.

B. SIMULATION RESULTS

The force tracking trajectory vibrates on planes, a slope and in sine working conditions as shown Figure 8 (a), Figure 9 (a) and Figure 10 (a), respectively, with a time ranging from 0–1s. Meanwhile, the corresponding performance of the force tracking error is highlighted in Figure 8(b), Figure 9(b) and Figure 10(b) from 1–5s.

By comparing the HI ($\sigma = 0$), AHI ($\sigma = 0.01$ and $\sigma = 0.05$), and DAHI controllers, the force has a stronger vibration and larger overshoots with a larger update rate σ at contact stage. HI and DAHI all have superior force overshoots suppression ability than AHI. However, at the stable stage, the compensated force tracking error is smaller when the update rate is larger. AHI and DAHI all have better force tracking ability than HI. The reason why DAHI controller can achieve both a small force overshoots and high accurate force tracking effects is that it is able to achieve dynamic adjustment update rate. The dynamic update rate of the DAHI controller is displayed in Figure 11. It can be clearly seen that the update rate is relatively small at $0 - 1$s when the force

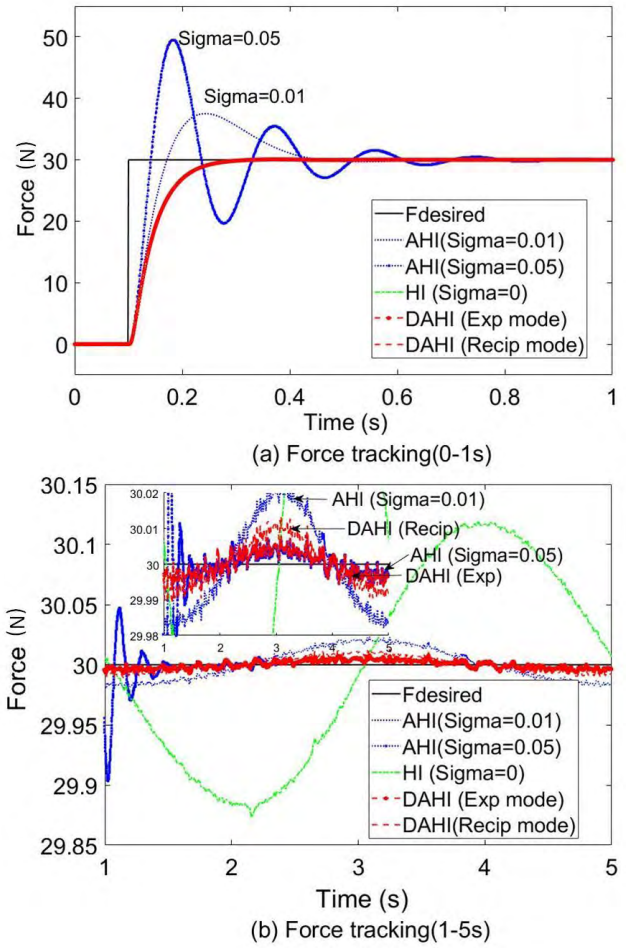

FIGURE 8. Performance comparison of HI, AHI and DAHI for force tracking on planes.

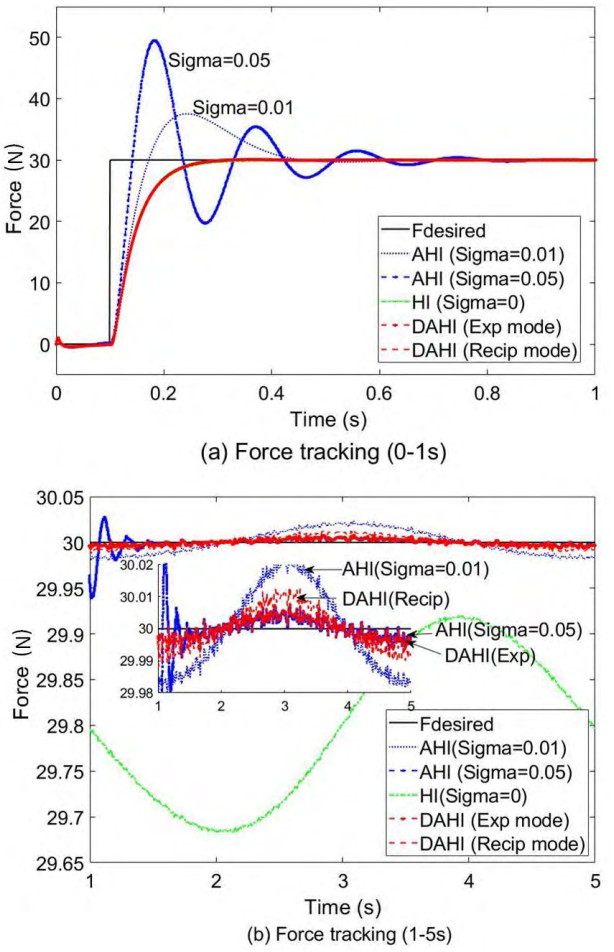

FIGURE 9. Performance comparison of HI, AHI and DAHI for force tracking on a slope surface.

error is large, and then gradually increased as the force error decreased at $1-5$ s.

As the environment becomes more and more complex (from flat planes to a sine surface), the force tracking error becomes larger and larger for HI controller. Both AHI and DAHI control have excellent force tracking ability to cope with environmental changes, so they can achieve better force tracking performance under complex environment. By comparing the results of AHI and DAHI, the force tracking effects of DAHI (Recip mode) is between the AHI ($\sigma = 0.01$) and AHI ($\sigma = 0.05$) on planes and slope surface. On a sine surface, DAHI (Recip mode) has a worse force tracking effects. Another interesting result can be found that DAHI (Exp mode) can follows closely with AHI ($\sigma = 0.05$) in any case.

From the simulation results, it is clearly shown that, DAHI control is superior in aspects of avoiding force overshoots than AHI control at the contact stage, as well as keeping force tracking error than HI control at the steady force tracking stage under condition of the complexity tracking surface and changeable stiffness environment. Beyond that, DAHI (Exp mode) has the same excellent ability as AHI in the force tracking under complex dynamic environment.

V. EXPERIMENTAL VALIDATION

A. EXPERIMENT SETUP

In order to verify the actual performance of the proposed dynamic adaptive hybrid impedance control method, three experimental studies were carried out to test the feasibility of a practical application. The experiments were conducted based on a simplified dynamic support system, and Figure 12 shows the experimental setup.

The experimental verification was conducted using the 2 DOF industrial manipulator shown in Figure 13. This manipulator was developed in our laboratory. For the operation of DC servo motor at each joint of the manipulator, an EtherCAT card is installed in an industrial PC that communicates commands between the controller and motor servo drives. Windows is used as the main operating system, and real-time operation is thus confirmed using a CODESYS Runtime module (soft PLC). The control period is set at $4ms$. The development of control program is written by CODESYS development environment and downloaded into the soft PLC. In order to achieve polishing for 2 DOF manipulator, a roller is installed on the end-effector behind the force sensor. A 3-Aixs force sensor is used to sense the external contact

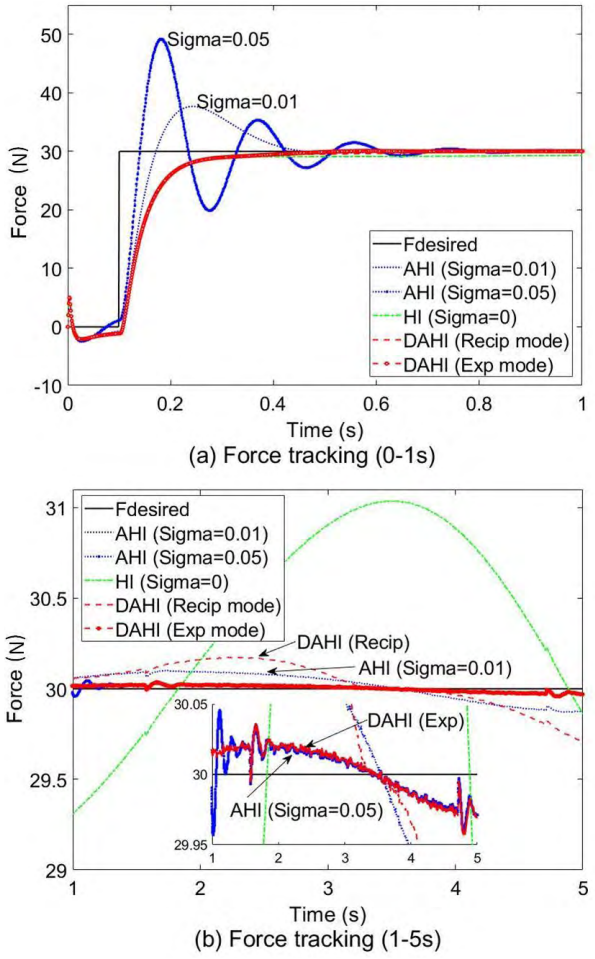

FIGURE 10. Performance comparison of HI, AHI and DAHI for force tracking on a sine surface.

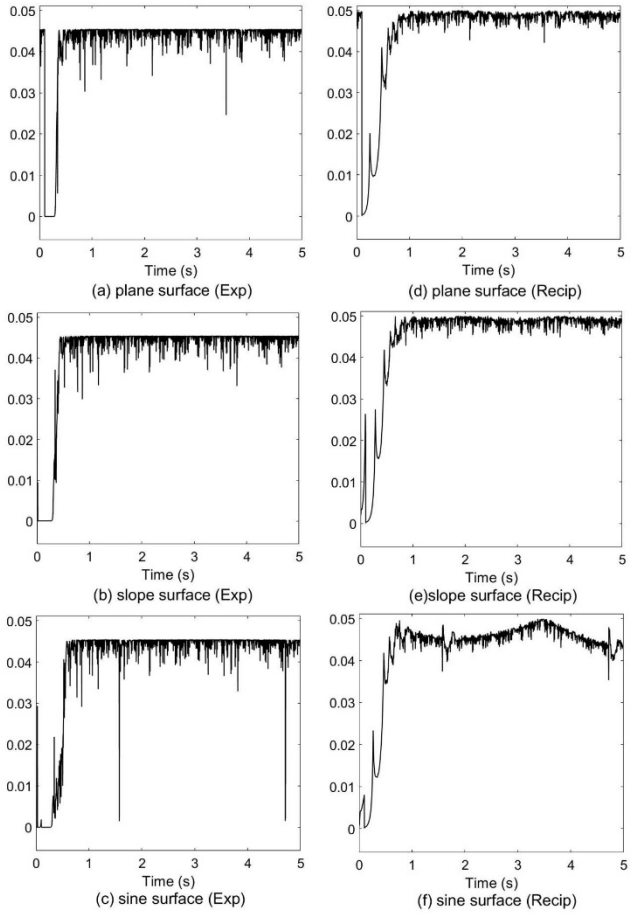

FIGURE 11. Dynamic sigma of DAHI controllers in the simulation. It can be seen that DAHI (Exp mode) is more robust than DAHI (Recip mode) in a dynamic environment.

force signals which are transmitted through Modbus-RTU communication mode.

The parameters of the basic impedance controller are set as following:$m_d = 1$ Ns^2/m, $b_d = 450$ Ns/m and $k_d = 0$. The maximum value of σ in the experiment is 0.007, which is much smaller than (15) in order to keep the system stable. The dynamic supporting system can be described as follows: the thin-polishing part is simulated using a 500mm $\times$ 20 mm $\times$ 1mm steel tape, which is easily deformed. One side of the steel tape is held in place and the other end is a moving support which is achieved via a linear module. Besides, there is a spring to achieve elastic support at the moving side. The parameters related to dynamic environment are not used in the control system.

B. EXPERIMENT RESULTS

1) FIRST EXPERIMENT

The first experiment is built so that both sides of the steel tape are fixed and no elastic support. The performance of the HI, AHI and DAHI control algorithms were compared experimentally.

The movement of the manipulator is divided into two stages: the contact stage and the dynamic force tracking stage.

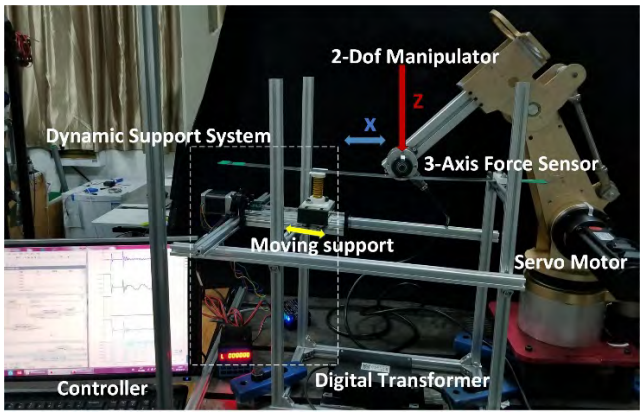

FIGURE 12. Experiment setup. The direction of the force control is on the z axis, and the position control is on the x axis.

At the contact stage (0–20s), which is shown in Figure 14, it moves along the surface in a normal direction, i.e. z axis direction to achieve the desired constant contact force. At the dynamic force tracking stage (20–50s) which can be seen in Figure 15, the desired constant contact force must be maintained in z axis while tracking the target moving trajectory on x axis.

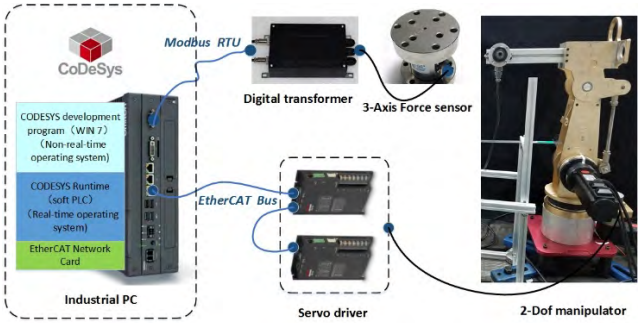

FIGURE 13. Hardware architecture of a 2-Dof manipulator control system.

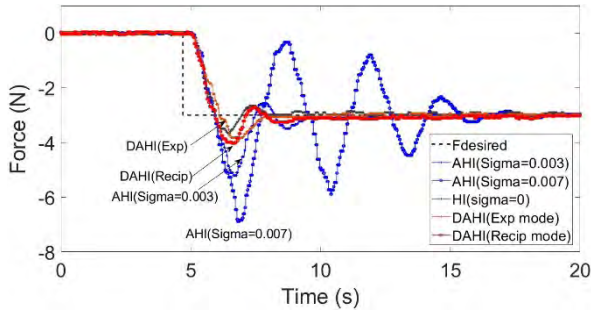

FIGURE 14. The contact performance of HI, AHI and DAHI are compared with fixed stiff support. DAHI has the superior force overshoot suppression ability compared with AHI.

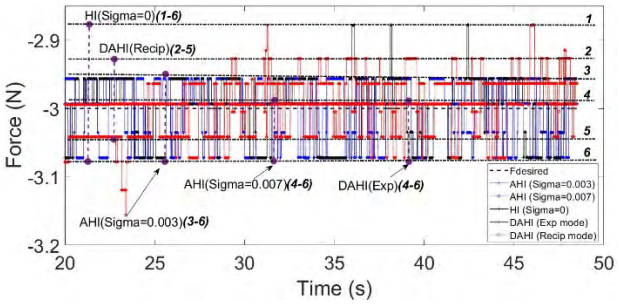

FIGURE 15. The dynamic force tracking performance of HI, AHI and DAHI are compared with fixed stiff support. DAHI has a superior dynamic force tracking ability compared with HI.

At the first stage, the AHI presents a great overshoot at the beginning of the convergence to the set force value $f_d = 3N$. Also, as σ increases, the force overshoots becomes more and more intense. This performance is similar to the simulation results. By contrast, DAHI (Recip and Exp mode) control algorithms show that the force overshoots in the contact stage clearly disappear which have the same effect that occurs with the HI control. Careful observation shows that DAHI (Exp) is more effective than DAHI (Recip) in terms of force overshoots suppression.

At the second stage, the AHI and the proposed DAHI control strategies can significantly improve the dynamic force tracking performance compared to the HI control strategy. The maximum force tracking errors is reduced markedly. By contrast, DAHI (Exp mode) has a better dynamic force

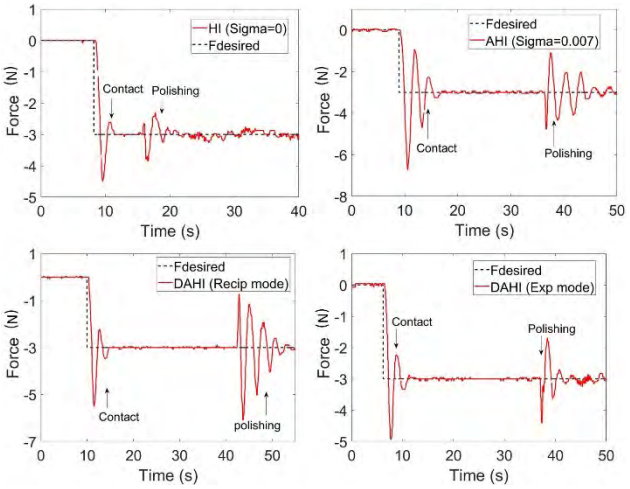

FIGURE 16. The contact performance of HI, AHI and DAHI are compared with fixed elastic support.

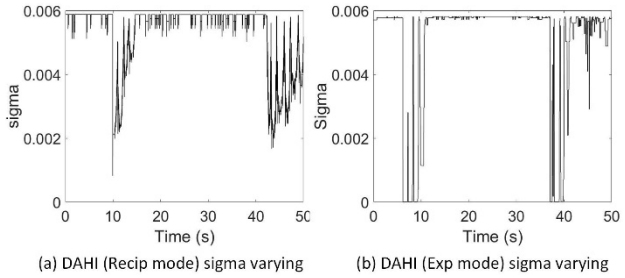

FIGURE 17. Dynamic sigma of the DAHI controller in the experiment. DAHI (Exp mode) has a larger adjusting range than DAHI (Recip mode) in a dynamic environment. In addition, DAHI (Exp mode) has a lower sigma value to avoid force overshoot in the contact stage.

tracking ability than DAHI (Recip mode). Furthermore, the result of DAHI (Exp mode) at dynamic tracking stage is similar to the AHI (Sigma = 0.007) experiment result.

2) SECOND EXPERIMENT

The second experiment is built so that one side of the steel tape is fixed, another side is fixed elastic support. The movement of the manipulator is also divided into the contact and dynamic force tracking stage.

At the contact stage, the experimental results are shown in Figure 16. The contact performance of the HI, AHI and DAHI control is similar to the first experiment. The difference is that at the beginning of polishing phase, the robot system will have an oscillation similar to the contact phase. The situation perhaps appears due to the effect of the elastic support. However, the oscillations were quickly suppressed in DAHI (Exp mode) and HI control strategies. Figure 17 demonstrates that the update rate σ changed with the DAHI controller. It can be seen that, DAHI (Exp mode) has a lower sigma value to avoid force overshoots than DAHI (Recip mode) in the contact stage.

At the dynamic force tracking stage which is shown in Figure 18, the AHI and the proposed DAHI control strategy

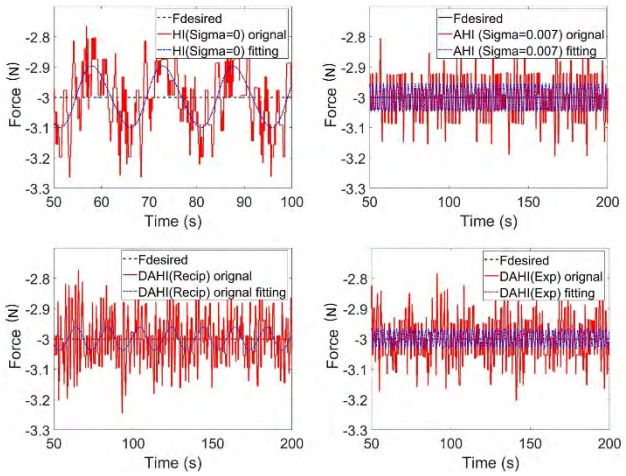

FIGURE 18. The dynamic force tracking performance of HI, AHI and DAHI are compared with fixed elastic support.

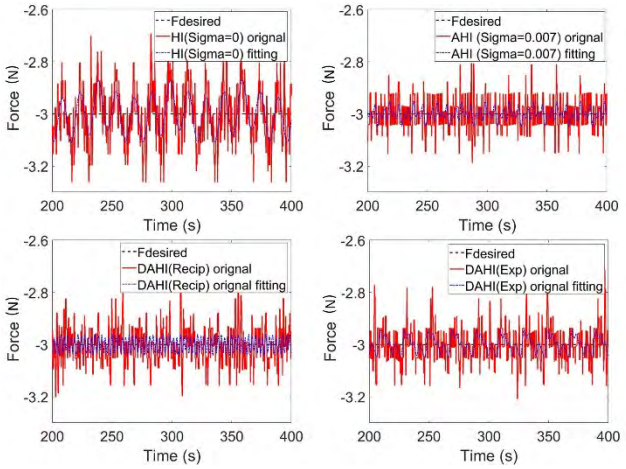

FIGURE 19. The dynamic force tracking performance of HI, AHI and DAHI are compared with a moving elastic support.

are still superior to HI control method. To make it easier to see the characteristics of the dynamic tracking force, the force tracking data is fitted with a Discrete Fourier fitting. It can be seen that DAHI (Exp) and AHI have the same trend at the force tracking stages. The results of the first experiment and the simulation are verified again.

3) THIRD EXPERIMENT

The third experiment is built to be more complex in that one side of the steel tape is fixed, but another is moving, albert with an elastic support. The moving process of the manipulator is the same as before experiments.

At the dynamic force tracking stage, as shown in Figure 19. Compared with the HI control, AHI and DAHI control all have a superior ability to cope with environmental changes namely, the ability to maintain force tracking. The force tracking performance of the HI AHI and DAHI controllers are similar to the above experiments. From the Fourier fitting trend, the effects of DAHI (Exp) and AHI control still have the same varying trend in a dynamic elastic support environment. The three experiments and simulations all verify that DAHI (Exp) has the accuracy force tracking ability as AHI at the steady force tracking stage.

VI. CONCLUSION

The importance of robot contact operation has been more and more important recently due to the introduction of interactive robots. A dynamic adaptive hybrid impedance (DAHI) controller to deal with dynamic contact force tracking in uncertain environment (e.g., polishing tasks) was proposed in this paper. The performances about transient response and steady-state error of hybrid impedance (HI) and adaptive hybrid impedance (AHI) control were analyzed, and the necessity of update rate dynamic adaptation is pointed out in this paper. A dynamic algorithm (two ways) computing the update rate on-line, was applied both to improve the performance of the AHI controller. The stability and boundary of the DAHI controller is analyzed, and the engineering implementation process is clarified. The simulation and experiment results all show that DAHI can improve the dynamic force tracking performance significantly in an uncertain environment. Moreover, three experiments and simulations all verify that DAHI (Exp) has the superior force tracking ability as AHI at force tracking stage. Besides, the reported methodology can be extended for force control in other tasks where an unknown environment is easily deformed or manufacture requires force control based on industrial robots. It offers a lot of potential in the film precision processing field for industrial applications.

Experimental effects may be limited due to the following reasons: (1) Restrictions on the hardware: ADC (Resolution) and the bandwidth of the controller; (2) the problem of signal processing: filter design; (3) the model uncertainties and external disturbances, the experimental effect is not particularly ideal, but the experiment is sufficient and verifies the effectiveness of the control scheme.

In the future, we will make efforts to improve experimental conditions for better control effects, and finding the influence of DAHI parameters on control performance and optimizing the control effects. Meanwhile, we will develop the 6-axis industrial robot and apply the control architecture. We will also try to design a motor-current-based estimation of Cartesian contact forces and torques to reduce development costs for robotic manipulators industrial application.

REFERENCES

[1] H. Park, J. Park, D.-H. Lee, J.-H. Park, M.-H. Baeg, and J.-H. Bae, "Compliance-based robotic peg-in-hole assembly strategy without force feedback," *IEEE Trans. Ind. Electron.*, vol. 64, no. 8, pp. 6299–6309, Aug. 2017.

[2] B. Yao, Z. Zhou, L. Wang, W. Xu, L. Quan, and L. Aiming, "Sensorless and adaptive admittance control of industrial robot in physical human-robot interaction," *Robot. Comput.-Integr. Manuf.*, vol. 51, pp. 158–168, Jun. 2018.

[3] L. Chao, Z. Zhi, G. Xia, X. Xie, and Q. Zhu, "Efficient force control learning system for industrial robots based on variable impedance control," *Sensors*, vol. 18, no. 8, p. 2539, 2018.

[4] F. Chen, H. Zhao, D. Li, L. Chen, C. Tan, and H. Ding, "Contact force control and vibration suppression in robotic polishing with a smart end effector," *Robot. Comput.-Integr. Manuf.*, vol. 57, pp. 391–403, Jun. 2019.

[5] L. Gracia, J. E. Solanes, P. Muñoz-Benavent, J. V. Miro, C. Perez-Vidal, and J. Tornero, "A sliding mode control architecture for human-manipulator cooperative surface treatment tasks," in *Proc. IEEE/RSJ Int. Conf. Intell. Robots Syst.*, Oct. 2018, pp. 1318–1325.
[6] J. E. Solanes, L. Gracia, P. Muñoz-Benavent, A. Esparza, J. V. Miro, and J. Tornero, "Adaptive robust control and admittance control for contact-driven robotic surface conditioning," *Robot. Comput.-Integr. Manuf.*, vol. 54, pp. 115–132, Dec. 2018.
[7] S. G. Yuen, D. P. Perrin, N. V. Vasilyev, P. J. D. Nido, and R. D. Howe, "Force tracking with feed-forward motion estimation for beating heart surgery," *IEEE Trans. Robot.*, vol. 26, no. 5, pp. 888–896, Oct. 2010.
[8] A. Q. L. Keemink, H. Van Der Kooij, and A. H. A. Stienen, "Admittance control for physical human–robot interaction," *Int. J. Robot. Res.*, vol. 37, no. 11, pp. 1421–1444, 2018.
[9] Z. Li, H. Bo, Z. Ye, M. Deng, and C. Yang, "Physical human–robot interaction of a robotic exoskeleton by admittance control," *IEEE Trans. Ind. Electron.*, vol. 65, no. 12, pp. 9614–9624, Dec. 2018.
[10] M. H. Raibert and J. J. Craig, "Hybrid position/force control of manipulators," *J. Dyn. Syst., Meas., Control*, vol. 103, no. 2, pp. 126–133, 1981.
[11] M. T. Mason, "Compliance and force control for computer controlled manipulators," *IEEE Trans. Syst., Man, Cybern.*, vol. SMCC-11, no. 6, pp. 418–432, Jun. 1981.
[12] N. Hogan, "Impedance control: An approach to manipulation: Part I—Theory," *J. Dyn. Syst. Meas. Control-Trans. Asme*, vol. 107, no. 1, pp. 1–7, 1985.
[13] N. Hogan, "Impedance control: An approach to manipulation: Part II—Implementation," *J. Dyn. Syst. Meas. Control-Trans. Asme*, vol. 107, no. 1, pp. 8–16, 1985.
[14] N. Hogan, "Impedance control: An approach to manipulation: Part III—Applications," *J. Dyn. Syst. Meas. Control-Trans. Asme*, vol. 107, no. 1, pp. 17–24, 1985.
[15] K. Bilal, M. R. Pac, C. Clévy, D. O. Popa, and P. Lutz, "Explicit force control VS impedance control for micromanipulation," in *Proc. ASME Int. Design Eng. Tech. Conf. Comput. Inf. Eng. Conf.*, Portland, OR, USA, 2013, pp. 1–8.
[16] J. Li, L. Liu, Y. Wang, and W. Liang, "Adaptive hybrid impedance control of robot manipulators with robustness against environment's uncertainties," in *Proc. IEEE Int. Conf. Mechatron. Automat. (ICMA)*, Beijing, China, Aug. 2015, pp. 1846–1851.
[17] M. Hosseinzadeh, P. Aghabalaie, H. A. Talebi, and M. Shafie, "Adaptive hybrid impedance control of robotic manipulators," in *Proc. 36th Annu. Conf. IEEE Ind. Electron. Soc.*, Glendale, AZ, USA, Nov. 2010, pp. 1442–1446.
[18] L. J. Love and W. J. Book, "Environment estimation for enhanced impedance control," in *Proc. IEEE Int. Conf. Robot. Autom.*, Nagoya, Japan, Nov. 1995, pp. 21–27.
[19] D. Erickson, M. Weber, and I. Sharf, "Contact stiffness and damping estimation for robotic systems," *Int. J. Robot. Res.*, vol. 22, no. 1, pp. 41–57, Jan. 2003.
[20] G. S. Kanakis, F. Dimeas, G. A. Rovithakis, and Z. Doulgeri, "Prescribed contact establishment of a robot with a planar surface under position and stiffness uncertainties," *Robot. Auton. Syst.*, vol. 104, pp. 99–108, Jun. 2018.
[21] R. Carelli and R. Kelly, "An adaptive impedance/force controller for robot manipulators," *IEEE Trans. Autom. Control*, vol. 36, no. 8, pp. 967–971, Aug. 1991.
[22] X. Wang, Y. Wang, and Y. Xue, "Adaptive control of robotic deburring process based on impedance control," in *Proc. IEEE Int. Conf. Ind. Inform.*, Singapore, Aug. 2006, pp. 921–925.
[23] D. Matko, R. Kamnik, and T. Bajd, "Adaptive impedance force control of an industrial manipulator," in *Proc. IEEE Int. Symp. Ind. Electron.*, Bled, Slovenia, Jul. 1998, pp. 129–133.
[24] S. Jung, T. C. Hsia, and R. G. Bonitz, "Force tracking impedance control of robot manipulators under unknown environment," *IEEE Trans. Control Syst. Technol.*, vol. 12, no. 3, pp. 474–483, May 2004.
[25] J. Duan, Y. Gan, M. Chen, and X. Dai, "Adaptive variable impedance control for dynamic contact force tracking in uncertain environment," *Robot. Auton. Syst.*, vol. 102, pp. 54–65, Apr. 2018.
[26] D. J. F. Heck, A. Saccon, N. van de Wouw, and H. Nijmeijer, "Switched position-force tracking control of a manipulator interacting with a stiff environment," in *Proc. Amer. Control Conf. (ACC)*, Chicago, IL, USA, Jul. 2015, pp. 4832–4837.
[27] B. Komati, C. Clévy, and P. Lutz, "Force tracking impedance control with unknown environment at the microscale," in *Proc. IEEE Int. Conf. Robot. Automat. (ICRA)*, Hong Kong, Jul. 2014, pp. 4832–4837.
[28] L. Roveda, N. Pedrocchi, M. Beschi, and L. M. Tosatti, "High-accuracy robotized industrial assembly task control schema with force overshoots avoidance," *Control Eng. Pract.*, vol. 71, pp. 142–153, Feb. 2018.
[29] L. Roveda, "Adaptive interaction controller for compliant robot base applications," *IEEE Access*, vol. 7, pp. 6553–6561, 2019.
[30] X. Sheng and X. Zhang, "Fuzzy adaptive hybrid impedance control for mirror milling system," *Mechatronics*, vol. 53, pp. 20–27, Aug. 2018.